energies

MDPI

Article

Effects of Ethanol Admixtures with Gasoline on Fuel Atomization Characteristics Using High-Pressure Injectors

Zbigniew Stępień [1], Ireneusz Pielecha [2,*], Filip Szwajca [2] and Wojciech Cieślik [2]

[1] Oil and Gas Institute—National Research Institute, 31-503 Krakow, Poland; stepien@inig.pl
[2] Faculty of Civil and Transport Engineering, Poznan University of Technology, 60-965 Poznan, Poland; filip.szwajca@put.poznan.pl (F.S.); wojciech.cieslik@put.poznan.pl (W.C.)
* Correspondence: ireneusz.pielecha@put.poznan.pl

Abstract: Correct fuel atomization is an important parameter in the process of preparing a combustible mixture. Distortions of the atomization can lead to unfavorable effects in the combustion process. This paper presents an analysis of the fuel atomization characteristics of high-pressure fuel injector tests. Optically tested injectors were previously tested in a 48 h engine test carried out in accordance with the CEC F-113-KC procedure, using alternative fuels with ethanol blends. As a result of engine tests on fuels containing various amounts of ethanol admixture, the injectors became contaminated. The effect of the deposits on the geometric atomization indicators was determined. This paper focuses on analyzing the area of the atomized spray in a constant volume chamber at different parameters, reflecting real operating conditions. We found that the addition of ethanol (20%) increases the observed spray area for all test points. Complementing the quantitative results is a qualitative analysis of fuel atomization for injector tests previously run on varying fuels.

Keywords: SI combustion engine; optical measurements of fuel atomization; high-pressure injectors; ethanol admixture; injector deposits; fuel atomization quality

Citation: Stępień, Z.; Pielecha, I.; Szwajca, F.; Cieślik, W. Effects of Ethanol Admixtures with Gasoline on Fuel Atomization Characteristics Using High-Pressure Injectors. *Energies* **2022**, *15*, 2926. https://doi.org/10.3390/en15082926

Academic Editors: Paweł Woś, Hubert Kuszewski and Albert Ratner

Received: 17 March 2022
Accepted: 13 April 2022
Published: 15 April 2022

1. Introduction

Fuel is an essential component of the automotive engineering process, which includes the selection of construction materials as well as fuel supply and storage systems. In addition to crude oil, biocomponents are also a significant part of the fuel industry [1]. According to the European Union's directives, increasing the share of so-called green energy is an important element of the climate and energy policy framework, which aims for a 40% reduction in greenhouse gases by 2030 [2]. An interesting bio-based fuel is alcohol, which can form a combustible mixture with petroleum products [3].

The physicochemical properties of the fuel can be used to outline the limits of engine regulation and optimization, especially with respect to the exhaust emissions of harmful components, performance, and vehicle utility. Fuel should guarantee technical functionality, appropriate function and operation, and maintain the vehicle's operational properties, including meeting the applicable exhaust emission norms throughout the engine's life cycle. Each change of fuels on the market must be adapted to the existing fleet of vehicles and their specific requirements. This also applies to the ethanol content in gasoline.

Fuels for internal combustion piston engines are characterized by functional properties that meet the stringent requirements of modern combustion engines. They enable the implementation of complex combustion process strategies in engines equipped with systems such as multiport fuel injection, turbo boost, catalytic reactors, and other exhaust aftertreatment systems. The chemical formulae of commercial fuels are constantly being improved. This is mostly caused by the growing exhaust emission toxicity restrictions for gases emitted from the combustion of fuels, and is enabled by the continuous development of engines. These activities force automotive designers to introduce changes in the design

of vehicle supply, combustion, and exhaust aftertreatment systems. Fuel manufacturers are required to change the chemical formulae of their products in order to minimize the resulting exhaust emissions generated during fuel combustion. As a result of these changes, the use of biofuels and biocomponents in admixtures with conventional fuels is continuing to gain importance in the automotive sector.

The three main benefits of using pure ethanol as a fuel, or as a component of gasoline and ethanol blends, include reduced CO_2 emissions, improved anti-knock properties of the fuel due to the significantly higher octane number of ethanol compared to gasoline, and high oxygen content in ethanol. This enables more efficient fuel combustion and, thus, limits the amount of harmful exhaust components emitted, such as solid particles (in terms of particle number and mass), as well as other unregulated emissions. Table 1 presents a comparison of the physicochemical properties of bioethanol and motor gasoline.

Table 1. Comparison of the physicochemical properties of fuels [4,5].

Property	Ethanol	Gasoline
Chemical formula	C_2H_5OH	C_4 to C_{12}
Molecular weight (g/mol)	46.07	100–105
Carbon mass fraction (%(m/m))	52.2	85–88
Oxygen mass fraction (%(m/m))	34.7	0
Fuel density in 20 °C (kg/dm^3)	0.792	0.72–0.78
Viscosity (cSt)	1.52	0.4–0.9
Flammability limit in 20 °C (%(v/v))	3.3–19	1.0–8.0
Excess air ratio	9	14.5–14.7
Temperature of self-ignition (°C)	423	257
Heat of vaporization (kJ/kg)	910	330–400
Upper heating value (kJ/kg)	26,900	42,000–44,000
Lower heating value (kJ/l)	21,300	~32,000
Research octane number	120–135	90–100
Motor octane number	100–106	81–90
Cetane number	–	5–20

Fuels containing ethanol open up potential uses of new technologies in the construction of internal combustion engines. These new technologies include downsizing, direct fuel injection [6,7], increasing the pressure of the fuel dose in the combustion chambers (boost), accelerating the ignition of the dose [8], and the development of the HCCI (homogeneous charge compression ignition) system and controlling CAI (controlled auto-ignition) [9].

Similarly to conventional gasoline, ethanol fuels tend to form harmful deposits on engine components, including on inlet ducts, outside/inside fuel injectors [10,11], on intake valves, and in combustion chambers [12–15].

Such deposits disturb the quantitative and qualitative processes of combustible mixture formation in the engine cylinders, leading to a decrease in performance and operational properties. Moreover, this also results in increased fuel consumption and exhaust emissions.

Both the external deposits—such as coke—and the internal injector deposits have a direct impact on the size and flow of the outgoing fuel mass spray and the degree of its atomization. This can cause uncontrolled and unpredictable changes in the excess air ratio of the combustible mixture formed, as well as other related consequences. In the case of multipoint fuel injection (MPFI) systems, the fuel jets of individual injectors—distorted due to the presence of deposits—flow over the walls of the intake system channels. A drop in the fuel atomization quality and differences in the intensity of fuel supply to individual cylinders result in increasing, uncontrolled changes in the composition of the fuel mixture formed in each of the engine cylinders. On the other hand, internal deposits will disrupt the injectors' control process and, thus, delay their reaction to changes in the provided control signal, thus resulting in both temporary and quantitative disturbances in the fuel dose supply to the cylinders, in relation to the requirements resulting from the selected combustion process strategy and the proper functioning of the exhaust aftertreatment system. The wear and tear of the injectors is also important in this context [16].

In contrast to engines with indirect injection, such as the SPI or MPFI types, in engines with direct injection—such as GDI engines—deposits on the injectors can also form in conditions under regular engine operating parameters. GDI engines use injectors that are located directly in the combustion chambers. Depending on the method of injector mounting, the formation of a stratified charge of the combustible mixture may be achieved by directing the atomized fuel spray reflected from the appropriately shaped piston crown (wall-guided) near the spark plug. The fuel can also be injected into a suitably shaped air vortex in the cylinder that carries the fuel spray near the spark plug (air-guided). The third method is to directly aim the fuel flow from the injector towards the spark plug (spray-guided). Coke deposits formed at the injector tip can distort the fuel spray, influencing both their spatial atomization and their overall range [17]. This has a very unfavorable effect on the process of the combustible mixture's formation, as well as the combustion process itself, in the combustion chamber of the engine. At the same time, an increase in the average size of the atomized fuel droplets can also be observed, which slows down the process of the fuel–air mixture's formation. The increase in the movement resistance of the injector needle disrupts the timing and the course of the opening and closing cycles of the gasoline injector in relation to the electrical impulse controlling the injector's operation. As a result, all of these problems reduce engine efficiency and performance, while increasing exhaust emissions and fuel consumption [18].

High temperature has a decisive impact on the deposit formation processes at the injector tips in the case of diesel engines with direct fuel injection. This depends not only on the engine's operating conditions (especially the engine load), but also on the placement of the injector location in the combustion chamber, and the efficiency of chamber heat removal. Central installation of the fuel injector in the combustion chamber of a GDI engine causes its greater heating (up to about 180–200 °C). This temperature is about 15–20 °C higher than when the injector is placed on the side of the combustion chamber, away from the exhaust valve [15]. An injector located on the chamber's side is often additionally cooled by the air supplied to the combustion chamber via the inlet valve or valves. The formation of deposits is also promoted by greater content of olefins in the fuel, as well as the direct impact of gases from the burned mixture in the engine chambers, along with high pressure. Deposits typically begin to form near the fuel injector holes and then, over time, they extend into the channels of the injector holes—especially on surfaces where fuel remains after the injection process has ended.

Generally, such deposits are the result of the fuel's thermal oxidation and polymerization processes, depositing in the form of carbon and oxygen moieties similar to wax or resin. Their formation requires high temperature—higher than the T90 of the fuel, which means the evaporation temperature of 90% of the batch fuel. Under such conditions, the fuel remaining in the injector channels after injection is completed evaporates, creating sediment precursors on the surfaces of the channels. If the fuel does not completely evaporate by the start of the next injection, these precursors are easily washed away, and no deposits are formed. However, if the fuel does evaporate completely (such as due to longer engine shutdown time), the precursors strongly stick to the surface, initiating the formation of deposits. The rate of deposit growth is influenced by the surface temperature of the injector channels, the fuel's flow rate through the injector holes after the engine starts, the temperature of the injected fuel, and the surface smoothness of the injector channels [19].

In the case of mixtures of pure gasoline with ethanol, as the proportion of ethanol in the fuel increases, the amount of deposits formed on inlet valves and in the engine's combustion chambers gradually decreases slightly when compared to the amount of deposits formed by pure gasoline without ethanol or additives [12]. Alcohol, as a solvent, can wash deposits from elements and components of the fuel supply system, and transfer them to filters and other subcomponents of the fuel injection systems. Therefore, research was performed with the goal of conducting an analysis (for engine and out-of-engine test conditions) of the impact of ethanol contained in gasoline on the size of fuel injector deposits and their impact on the quality of fuel atomization.

In their review paper, Xu et al. [13] draw attention to the need to conduct work to identify the atomized fuel spray structure in GDI systems, with the use of optical methods—specifically high-speed image capture technology. In this way, the impact of the geometry of the injector outflow holes [20], control parameters [21], or contamination of the outflow holes [11], among others, could be determined.

Optical analysis of fuel atomization using a GDI injector, which worked for 30 h in stable conditions and with six cold starts, showed an increase in the range of all analyzed fuel sprays, and a significant increase in the mean droplet diameter [22]. Moreover, photos of the injector outflow holes after the test, taken with a SEM microscope, showed the formation of deposits not only on the outside, but also on the inside of the injector channels. In the subsequent optical tests [23], which tested injectors that had operated for 55 h during an engine test, the injection start was found to be delayed by 0.03 ms compared to new injectors. In this article, the authors use fast-speed filming to assess structural changes in the injected fuel spray as a result of using DI injectors supplied with fuel with varied levels of ethanol content.

The aim of this research is to evaluate the effects of gasoline injectors that have been fed with different fuels. Thus, this work does not analyze the atomization changes of doped fuels, but only the effects caused by such flows.

2. Test Objects and Methods

2.1. Fuels

Three gasolines were used in the engine tests, including pure gasoline with a high tendency to create engine deposits, and two blends of gasoline mixed with 10% (*v*/*v*) and 20% (*v*/*v*) ethanol. The reference fuel RF-12-09 batch 10 used in the CEC engine tests was adopted as the pure (reference) gasoline. This type of gasoline was used as the reference fuel because it was the most commonly used variant in many engine tests conducted by various European laboratories. The physicochemical properties of the fuel samples prepared for the tests are presented in Table 2.

Table 2. Physicochemical properties of gasoline samples prepared for engine testing (authors' research).

Property	Unit	RF-12-09 Batch 10	RF-12-09 Batch 10 +10% (*v*/*v*) Ethanol	RF-12-09 +20% (*v*/*v*) Ethanol	Test Procedure
Density at 15 °C	kg/m^3	746.3 ± 0.4	758.2 ± 0.4	751.7 ± 0.4	PN-EN ISO 12185:2002
Research octane number	-	96.0	97.4	98.2	PN-EN ISO 5164
Motor octane number	-	85.9	86.4	87.8	PN-EN ISO 5163
Sulfur content	mg/kg	9.0 ± 1.5	7.8 ± 1.7	5.3 ± 1.7	PN-EN ISO 20846:2020
Content of hydrocarbon types:					PN-EN 15553:2009
Olefinic	% (*v*/*v*)	7.4 ± 1.4	5.7 ± 1.4	5.1 ± 1.1	
Aromatic	% (*v*/*v*)	32.1 ± 2.6	30.4 ± 2.6	28.8 ± 2.6	
Benzene	% (*v*/*v*)	0.5 ± 0.1	0.4 ± 0.1	0.3 ± 0.1	PN-EN 238:2000 + A1:2008
Oxygen	% (m/m)	0.11	3.73 ± 0.29	7.40	PN-EN 1601:2017-09
Organic compounds containing oxygen:					PN-EN 1601:2009
Methanol	% (*v*/*v*)	<0.80	<0.17	<0.17	
Ethanol	% (*v*/*v*)	<0.80	10.2 ± 0.57	20.1	
Fractional composition:					PN-EN ISO + 3405:2019
T10	°C	52.3 ± 2.6	53.0 ± 2.6	51.4 ± 2.6	
T50	°C	106.5 ± 3.6	100.8 ± 3.1	72.4 ± 3.1	
T90	°C	172.9 ± 4.0	171.9 ± 4.0	163.4 ± 4.0	

2.2. Research Method

2.2.1. Engine Tests

Fuel tests were performed on an engine test stand in accordance with the CEC F-113-KC test procedure, in which the 1.4 L displacement VW EA111 BLG engine was used as the test engine (Figure 1).

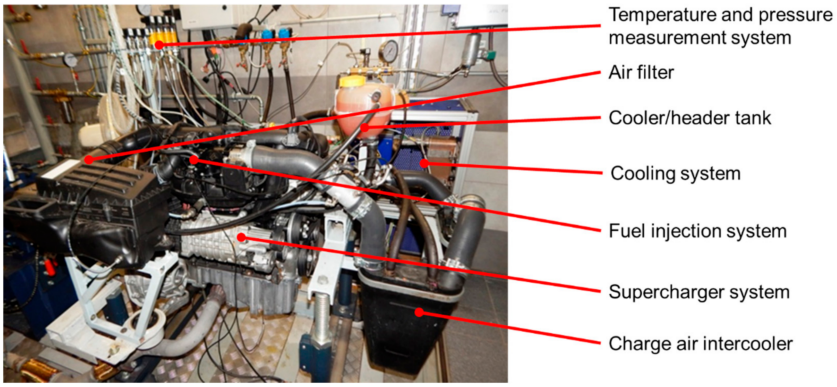

Figure 1. Image of the test stand with the VW EA111 BLG engine (photo INIG–PIB).

The duration of the "Keep-Clean" test was 48 h. In this test, the engine was operated under steady-state conditions, with a rotational speed of 2000 rpm and a load of 56 Nm. The engine control system was modified to achieve a constant value of the excess air ratio for the stoichiometric mixture. The test allowed for the assessment of the reference or blended fuel (gasoline) in terms of the fuel injector's sedimentation tendency. The engine featured wall-guided, 6-hole, electromagnetic fuel injectors. One of the hallmarks of wall-guided systems is the lateral location of the fuel injector in the engine combustion chamber.

Usually, the fuel injector is located below the air inlet to the combustion chamber. The fuel evaluation criterion in the tests was the changing width of the electric impulse that controls the fuel injection time. This time changes (increases) as the amount of sediment accumulating inside and outside of the injectors gradually grows. The result, which was the difference in the length of the electric pulse related to the duration of a single fuel injection measured at the end and at the beginning of the test, was given as a percentage. Taking into account the unstable nature of the changes in injection time during the test, a methodology based on a trend line was used to estimate the length of the injection time control pulse.

2.2.2. Optical Tests with the Use of a Constant Volume Chamber

Optical studies of engine processes focused on the analysis of the fuel mixture formation and combustion processes [24,25] make it possible to identify the basics of the phenomena, the effects of which were obtained using continuously running engines. A constant volume chamber that simulated the conditions of static fuel atomization was used to evaluate the qualitative indicators of fuel spray from high-pressure injectors for the purposes of this article.

It was assumed that in constant volume chamber tests the impact of the piston movement and thermal changes of the gas inside the chamber on the analyzed phenomenon was negligible. Such assumptions were made for the optical tests of the fuel injection process performed in static conditions.

The cube-shaped chamber was equipped with holes in each wall where translucent quartz windows were placed, a mounting system for attaching a simplified engine head (injector mount), valves supplying and discharging gas (air) to the chamber, and a heating system using heaters located in the corners of the cube.

The constant volume chamber used in the tests is shown in Figure 2. The test setup consisted of control and recording equipment, including the HSD V711 systems for deter-

mining the injection sequence and activating the camera, the HSS5 LaVision system for recording images, and the AVL IndiMicro system for recording rapidly varying parameters. Detailed information about the experimental setup is shown in Table 3.

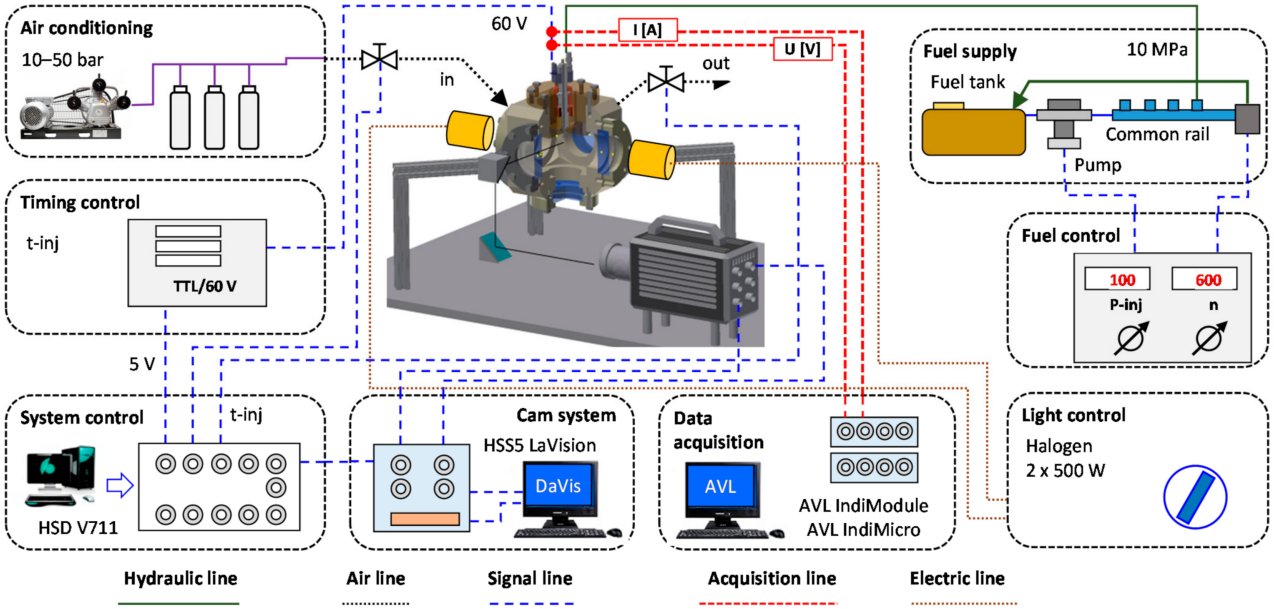

Figure 2. Test stand (constant volume chamber) for the assessment of fuel spray injection.

Table 3. Adjustment parameters used during optical testing with the constant volume chamber.

Parameter	Value
Injection pressure	10 MPa
Injection pump speed	600 rpm
Backpressure (relative)	0; 0.1; 0.2 MPa
Injection time	0.4 and 0.6 ms
Imaging resolution	512 × 512 px
Frame rate	10 kHz
Illumination power	1 kW

The constant volume chamber can be used for tests with a back pressure of 8 MPa; however, in the presented analyses, this pressure was kept in the range from 0 to 0.2 MPa relative pressure, corresponding to the pressure prevailing in the standard operating conditions of the tested injectors.

The fuel (gasoline) was supplied to the injector by two high-pressure injection pumps mounted in the engine body. The pump system belonged to the BMW M4 GTS sports car engine.

A LaVision High-Speed Star 5 recording camera was used to capture the fuel atomization images. Image recording took place at a frame rate of up to 10,000 Hz (10,000 fps). The optical configuration of the camera for fuel atomization tests is shown in Figure 2. The research used a fixed-focus AF Nikkor lens.

The fuel atomization tests were carried out with the use of standard continuous lighting with a halogen lamp. No optical filter was used to record the images, as only the light from the halogen lamp reflected from the injected fuel droplets was recorded. The light was not filtered, oriented, or bundled. The recorded light reflected from the fuel spray droplets was refracted on the droplets in the entire illuminated volume of the chamber.

The analysis of the fuel injectors' operational parameters was determined based on the optical tests of fuel spray atomization. The scope of this work included:

- Photographic documentation (high-speed camera with f = 10–50 kHz);

- Linear spray range assessment;
- Assessment of the sprayed fuel's surface area (parallel to the injector axis).

The results were analyzed using LaVision's DaVis software. A procedure was adopted to determine the geometric parameters of the fuel spray, which involved subtracting the background photo from the fuel spray photo taken (the initial image). As a result of this operation, the difference in light recorded in the two photos (the new and the initial) was obtained. Then, the mask (image area) was established, which was the area used for further analysis (Figure 3). In this methodology, the spray angle was omitted, due to the inability to isolate a single fuel jet.

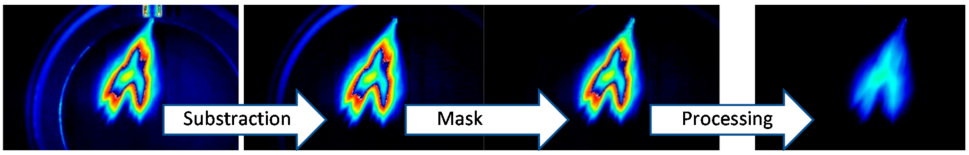

Figure 3. The image processing method using the DaVis software.

Geometric parameters of the fuel spray were determined using the following algorithms:

- Spray range—based on the X coordinate (change in the number of pixels in the vertical direction, without angular changes in the position of the injectors; the criterion for this measurement was the luminance value for each pixel):

$$S = x_n - x_o \{x_n = \max(x_i); x_i{:}f(\text{luminance})\}, \quad (1)$$

- Spray area—based on the number of pixels in the measuring area (the criterion was the luminance value for each pixel):

$$A = \sum_{i=1}^{\max} x_i; \ \{xi{:}f(\text{luminance})\}, \quad (2)$$

The analysis of the geometric parameters was carried out as described in Table 4. The tests were conducted for four injectors, and each optical test was repeated twice. For each pressure case, 8 measurements were obtained. The maximum value of the jet overhang error did not exceed 9.8% from the averaged value; it was the highest at the smallest value of back pressure.

Table 4. The optical signal parameterization to determine the fuel spray's geometric parameters.

Characteristic	Image
Injection range: The global range was determined without using (for optical reasons) analysis of the individual fuel injections. The speed of the spray front was determined by dividing the current range by the time step between successive photos.	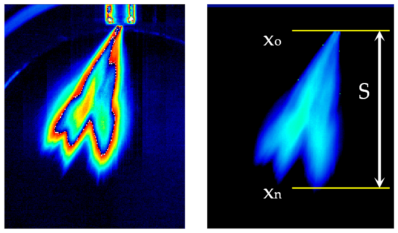
The spray area was defined as the number of pixels covering a specific area that had the accepted level of pixel luminous intensity.	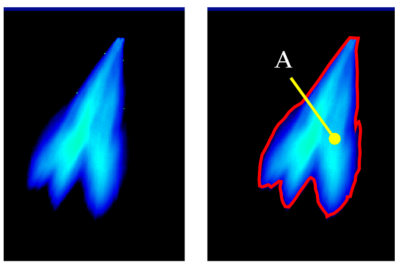

2.3. Scope of Research

The scope of engine tests included the use of three fuels:

- RF-12-09 batch 10 (reference untreated base fuel);
- RF-12-09 batch 10 + 10% (v/v) ethanol;
- RF-12-09 batch 10 + 20% (v/v) ethanol.

For the purposes of this procedure, the nomenclature of the fuel types was correlated with the nomenclature of the injectors on which they operated, as per Table 5.

Table 5. Nomenclature of injectors used for testing.

Type of Fuel	Injector Designation	Test Fuel
RF-12-09 batch 10 RF-12-09 batch 10 + 10% (v/v) ethanol RF-12-09 batch 10 + 20% (v/v) ethanol	Injector 1 (Inj_1) Injector 2 (Inj_2) Injector 3 (Inj_3)	Unleaded petrol 95; UFI: 8300-F0HA-000R-GE9C

Optical registration of the atomization of the fuel spray injected into the constant volume chamber (CVC) was carried out for 6 points (p1–p6). Three values of relative pressure (0, 0.1, and 0.2 MPa) were used in the constant volume chamber, constituting the back pressure for the injected fuel, and two pulse durations controlling the injector opening time (0.4 and 0.6 ms). The map of the measurement points used is shown in Figure 4a. The fuel was supplied to the injector at a constant pressure of 10 MPa by the high-pressure pump working at 600 rpm. A picture of the high-pressure injector is shown in Figure 4b, where the location of the outflow holes is marked.

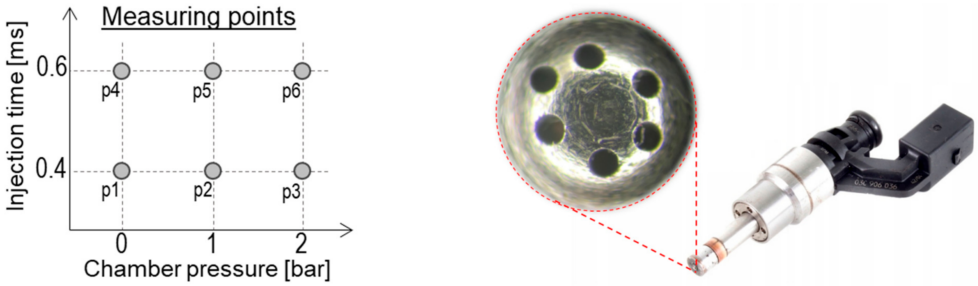

(**a**) (**b**)

Figure 4. Research methodology: (**a**) a map of the measuring points at which tests were conducted; (**b**) the arrangement of the injection nozzles on the injector.

3. Results

3.1. Assessment of Injector Deposits during Engine Tests

Figures 5 and 6 show the results of engine tests of three fuels, expressed as the percentage changes in the fuel injection time caused by the formation of injector deposits. Figure 5 shows the photos of the deposits formed on the tips of the fuel injector nozzles throughout the three tests. Figure 6 shows the results of changes in the fuel injection time (Figure 6a) and the percentage changes in the fuel injection time (Figure 6b) caused by the formation of injector deposits in tests carried out in accordance with the CEC F-113-KC procedure for the three tested fuels. A detailed analysis of changes throughout the test is presented in another article [26].

The tests carried out using the tested fuels led to the formation of deposits on the atomizer. Deposits accumulated near the tip of the injector atomizer, especially in the area of the fuel holes of the injector and inside the fuel outlet channels. As shown in Figure 5, the deposits observed after the tests on the fuels RF-12-09 and RF-02-09 + 20% ethanol indicated signs of corrosion. The deformation of the fuel outflow area was clearly observable in the photos of injector operation while running on the RF-12-09 fuel + 10% ethanol.

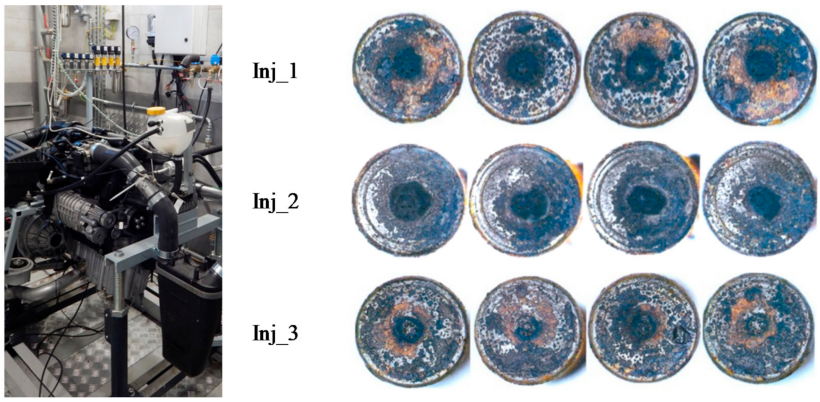

Figure 5. Injector contamination after the tests performed on the test engine.

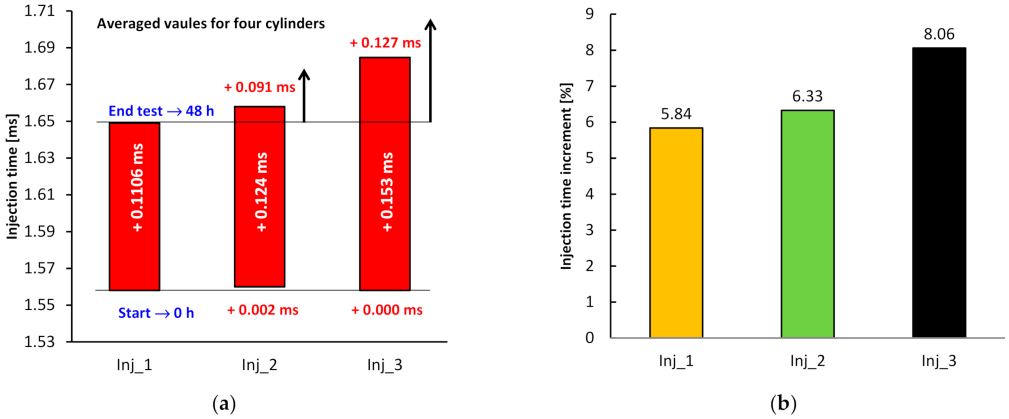

Figure 6. The conducted analysis of fuel injection time changes: (**a**) change in injection time; (**b**) percentage increase in injection time after a 48 h test.

Analysis of the dose correction parameters indicated an extended injection time for fuels with the admixture of ethanol. The injection time increase reached 0.127 ms at the end of the engine test cycle relative to the initial duration, which was an 8% correction from the dose at which the CEC F-113-KC test was initiated. However, considering that all of the analyzed fuels contributed to the need to introduce dose adjustments, the differences between the discussed fuels were found to be less, at up to 2%.

3.2. Evaluation of Results Obtained in the Constant Volume Chamber Tests

3.2.1. Fuel Atomization Tests with the Injection Time t = 0.4 ms

The previous tests of injectors and fuels carried out on an engine test stand were taken into account when performing the tests using a constant volume chamber.

Figure 7 shows a sequence of photos depicting the spread of the injected fuel spray, taken using the high-speed imaging techniques, for a back pressure of 0.1 MPa. The first photo was taken 0.1 ms after the injector was opened; hence, the time of 0.1 ms was assumed as the time after the start of injection (ASOI). The results were presented in three columns for the analyzed base fuel and the fuels with 10% and 20% ethanol. Considering the time when the injector needle was lifted—i.e., the first two photos—differences could be seen in the area covered by the outgoing fuel. The smallest area was obtained with the fuel flowing from the injector operating using the reference base fuel RF-12-09. The area increased successively with the increasing share of ethanol. At this stage, no significant differences in the shape of the spray were recorded. In subsequent time steps (frames), the geometry of the fuel spray cone for the injector fed with RF-12-09 + 20% ethanol changed. The fuel stream exiting the individual nozzles became distinguishable, in contrast to what was found for the injectors operating on the reference fuel. These differences are particularly

visible in the area of the jet head. A change also occurred in the fuel's distribution over the jet area, represented by the illumination intensity. This effect resulted from a change in the amounts of deposits on the inner walls of the outflow channels. The amount of embedded fouling within the orifices significantly affected the jet structure. Moreover, the change intensified with the change in alcohol concentration in the fuel on which the injector worked.

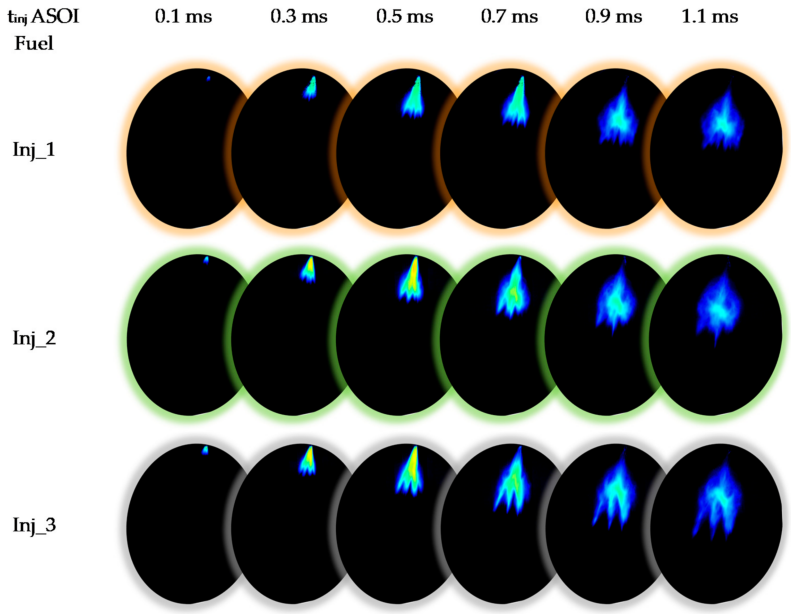

Figure 7. Fuel spray data of the tested RF-12-09 fuels with admixture (injection parameters: P_{inj} = 10 MPa, t_{inj} = 0.4 ms, P_b = 0.1 MPa).

The image of the spray geometry for a time step of 0.7 ms is shown in Figure 8. The color of the spray indicates the intensity of luminescence. The blue color shows the exposure area of a flat spray with a greater degree of atomization, while the yellow color shows the concentrated fuel. As a result of using fuel without ethanol admixture, the outflow channels of the injector were shaped in such a way as to obtain a more even distribution of the fuel in the stream, compared to injectors operating on fuels with ethanol admixture. Lower fuel concentration in the vicinity of the injector holes when using fuels with the admixture of ethanol indicates increased dynamics of the outflow.

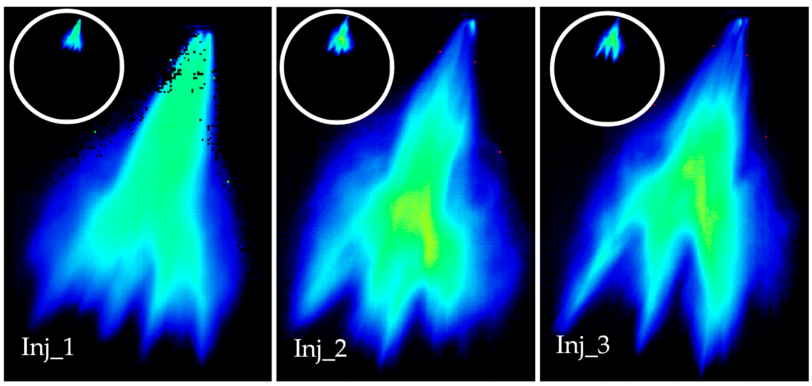

Figure 8. An example of fuel atomization tests for injection time 0.7 ms (P_{inj} = 10 MPa, P_b = 0.1 MPa, t_{inj} = 0.4 ms, f = 10 kHz, 512 × 512 px).

The presented spray penetration showed slight differences in all analyzed combinations, as shown in Figure 9. The individual differences between the maximum values

ranged from 2.6 to 3.2%, which was (as shown in Figure 6) in the range of ±1.2 mm. Since the ethanol admixture and the reference fuel produced such small variations, it was noted that the spray penetration analysis did not result in a significant differentiation of fuel properties. The obtained results, where the highest spray penetration was achieved for the fuel with 20% ethanol admixture, may be the result of the high variability in individual injections. Thus, this parameter is not used in the remaining portion of this article.

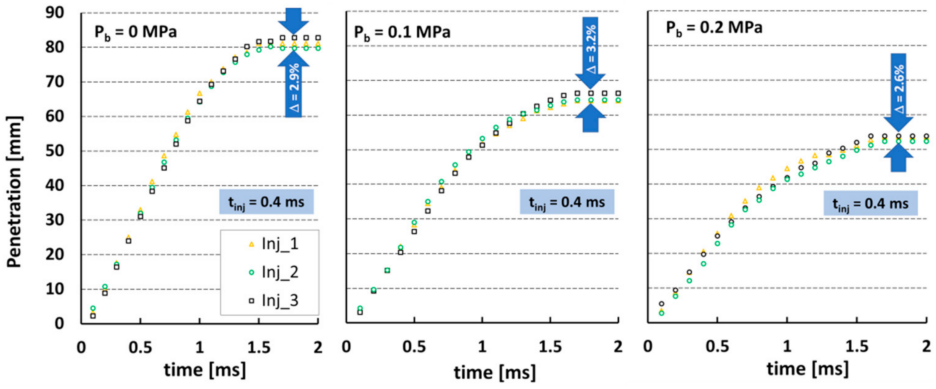

Figure 9. Fuel spray penetration for pure RF-12-09 fuel, as well as fuels with +10% ethanol and +20% ethanol admixture, at 0.4 ms injection time and various back pressure values.

Analysis of the fuel spray area's changes over time showed much greater variation in the tested cases, making it possible to assess the flow characteristics within the injectors. The addition of 20% ethanol, for all back pressure values, increased the surface area observed over time, as well as the highest surface area reached at the measuring point. The differences in the analyzed time interval of 2 ms after injection indicated a 10 to 33% increase in surface area in that time span.

With increasing back pressure, this characteristic became consistent, indicating that the greater the share of added ethanol, the greater the achieved fuel spray area (Figures 10 and 11). This trend was not observed only in the results obtained with no back pressure, where the reference fuel without admixture achieved a larger surface area than the fuel with 10% ethanol. These results, however, serve only to supplement the research data, and zero back pressure conditions do not occur in an operational combustion engine.

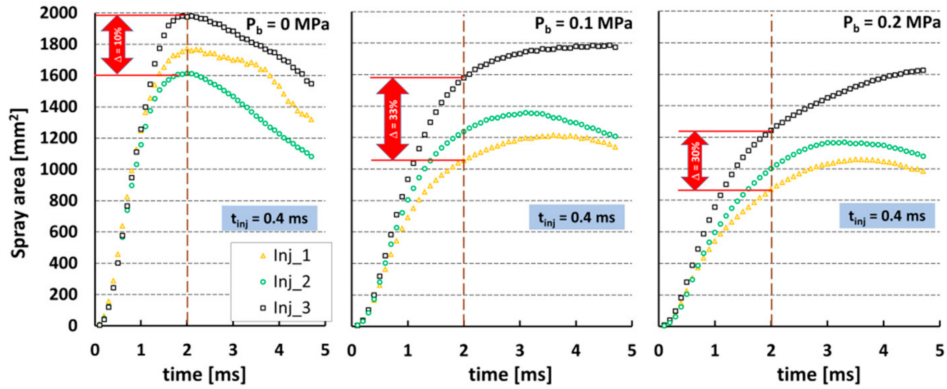

Figure 10. The fuel spray area related to the RF-12-09 03 (t_{inj} = 0.4 ms and P_b = 0; 0.1; 0.2 MPa; the results are mean values).

The similar penetrations obtained during the analysis indicate similar coking of the injector nozzles. This means that fuel modifications do not result in large injection time differences. Nevertheless, the injection time differences (Figure 6) were due to (1) different heating values of the doped fuels and (2) nozzle coking. The correlation of engine operation

with optical tests is complicated. In the engine, a constant value of the operating parameters had to be obtained (coking of the orifices forced an increase in the injection time). Optical tests were carried out with a constant value of the dose of the same fuel. If the penetration is quite similar, this means that the nozzle flow diameter is also approximately the same. However, the degradation of the profile along the length of the fuel outflow will be dissimilar. A larger spray area results in more hole degradation at the end of the fuel outflow. Increasing the test time from 48 h to 96 h would significantly improve the quality of the analyses obtained. However, typical test procedures assume shorter test times.

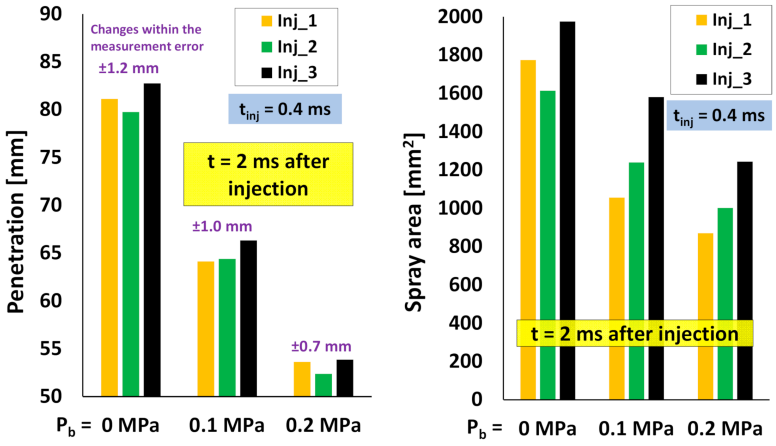

Figure 11. Summary of the average penetration and spray area at 2 ms for the RF-12-09 fuel and its versions with admixture.

3.2.2. Fuel Atomization Tests with the Injection Time t = 0.6 ms

Figure 12 presents a sequences of images of the fuel injection process taken for an injection time of 0.6 ms. As was observed with the tendencies relating to the fuel concentration in the exhaust gas for the injection time of 0.4 ms, the uniformity of fuel distribution in the spray area imaging also decreased with the increase in ethanol content in the fuel.

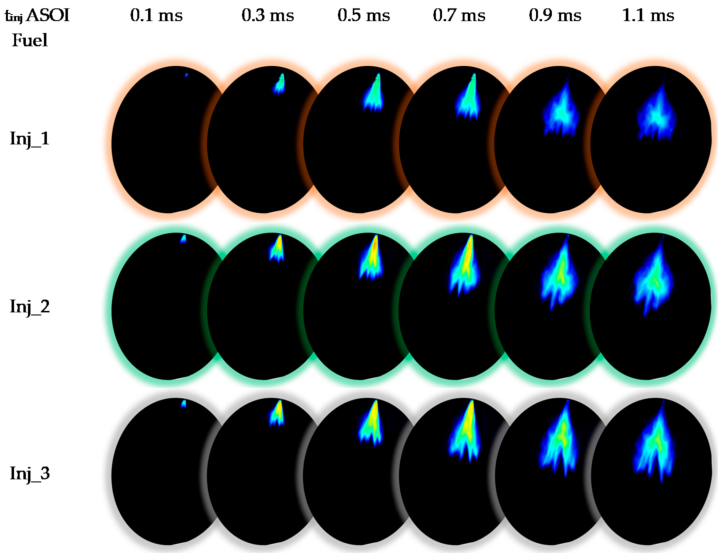

Figure 12. Fuel spray data of the tested RF-12-09 fuels with admixture (injection parameters: P_{inj} = 10 MPa, t_{inj} = 0.6 ms, P_b = 0.1 MPa).

After confirming the lack of notable differences in the injection range, the analysis of the changes in fuel spray parameters for varied lengths of injection time was performed based only on the surface area value (disregarding the fuel penetration data). The same

relationship was obtained for all of the analyzed back pressures in the constant volume chamber. Thus, it can be concluded that both the smallest maximum spray area and the smallest value at 2 ms after injection were achieved in the series 1 injector tests. These were subjected to engine tests running on the RF-12-09 fuel (Figure 13). Fuels with ethanol admixture were characterized by a change in the injection geometry, and optical tests of the injectors previously operating with these fuels indicated a 20% increase in the spray area compared to injectors used with fuels without ethanol admixture. The greater the back pressure in the constant volume chamber, the smaller the difference in the mean between the reference fuel and the fuel with 20% ethanol, reaching 13% for a 2 ms post-injection time and a back pressure of 0.2 MPa.

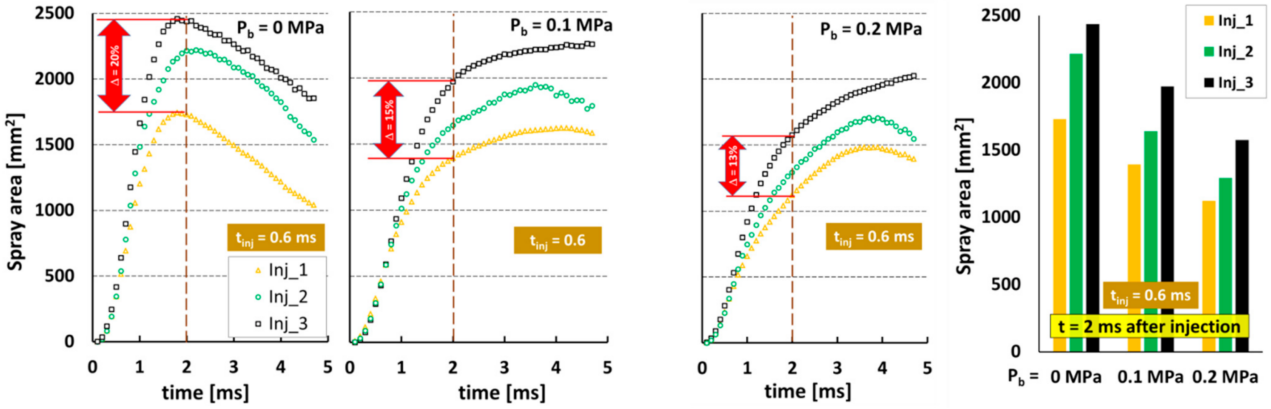

Figure 13. Spray area characteristics for increased injection time t_{inj} = 0.6 ms.

3.2.3. Contour Map Analysis

Results of the optical analysis for the maximum value of the spray area, which is a representative parameter, are presented in the form of contour maps (Figures 14 and 15). The maps were developed using the interpolation method—inverse distance weighting (IDW) in accordance with the following equation:

$$\hat{z}(x) = \frac{\sum_i^n w_i x_i}{\sum_i^n w_i} \quad (3)$$

where $\hat{z}(x)$ is the estimated value, w_i is the weighing function, and x_i is an interpolation point with a known value.

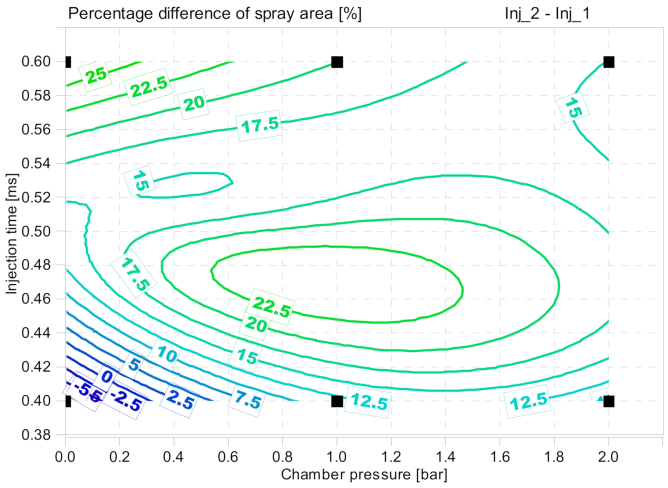

Figure 14. Contour map of the percentage variation in the spray area between injectors 2 and 1.

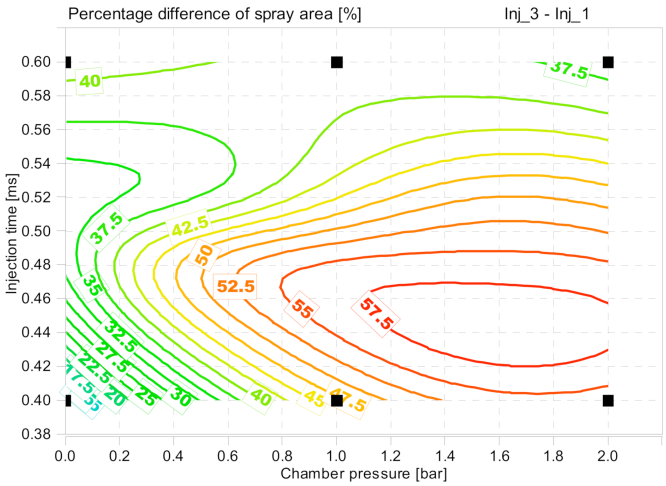

Figure 15. Contour map of the percentage variation in the spray area between injectors 3 and 1.

The area covered by the maps represents the percentage difference between the spray area of the fuel spray generated by the injector when using the RF-12-09 fuel with ethanol admixture (injectors 2 and 3) and the area generated with pure reference fuel (injector 1). The vertical axis shows the injection time, while the horizontal axis shows the pressure in the constant volume chamber, simulating the pressure present in the cylinder during fuel injection. The percentage difference is shown, assuming that positive values indicate an increase and negative values indicate a decrease in the maximum value of the spray area, in comparison to injector 1. The color blue indicates the smallest values, while red corresponds to the maximum differences.

Figure 14 shows the difference in the maximum area of injector 2's fuel spray relative to the area from injector 1. In a significant portion of the analyzed cases, a 10%, ethanol admixture resulted in changes in the outflow holes' geometry, increasing the maximum area covered by the fuel spray to 25%. The most notable differences were found for the maximum back pressure value as well as the injection time of 0.6 ms. The degree of atomization was found to decrease for low ambient pressure values and for the minimum value of the injection time.

Increasing the proportion of ethanol in the fuel in injector 3 doubled the maximum spray area in the entire operating range when compared to injector 2. The maximum difference was found to be less than 58%, which was more than double the value for injector 2. As found with injector 2, a clear tendency was observed where the spray area increased along with the values of back pressure and injection time.

For the analyzed fuel RF-12-09, the addition of ethanol changed the rheological properties, directly corresponding to the operational changes found in the injectors. The SI engine injectors running on fuel with alcohol additive showed a change in the atomization indicators compared to those operating on pure fuel within the range of relative back pressure of 0–0.2 MPa. The pressure range was close to that in the cylinder of a real engine.

4. Discussion

The research on the tendency of fuels to form deposits on fuel injectors was carried out in line with the specifications of the CEC F-113-KC test procedure, where the VW EA111 BLG engine was used as the test unit. It is important to note that each engine design, type of fuel injection used, mixture formation process, and combustion strategy has a significant impact on the process and intensity of the injector's deposit formation. Thus, they impact the final result of the fuel assessment obtained for the tendency of deposit formation, as well as the size of injector deposits produced over a given period of time. The conducted research focused on the assessment of the impact of an ethanol admixture (using two blends, i.e., 10% (v/v) and 20% (v/v)) on the tendency of injector deposit formation. The engine used for testing was not a flex-fuel engine type, and was therefore not adapted to operation

using fuels with ethanol in them, restricting the maximum level of alcohol admixture in the fuel. Comparative studies of ethanol and gasoline atomization [27] conducted with DI outward-opening injectors indicated a reduction in the fuel spray area and range when using ethanol. The spray velocity was also observed to be lower. The current tests were carried out using standard gasoline, so there was a difference in the tested medium.

By analyzing the engine test results presented in Figure 6b, it was found that the admixture of ethanol has a negative effect on counteracting the formation of injector deposits. The injection time was seen to increase throughout the testing of each of the following fuels:

- RF-12-09—injection time increased by 5.84%;
- RF-12-09 + 10% (v/v) ethanol—increase in injection time by 6.33%;
- RF-12-09 + 20% (v/v) ethanol—injection time increased by 8.06%.

These results were later confirmed by analyzing the images of deposits formed on the injector tips, as shown in Figure 5. The images of deposits on the injector tips after the engine tests were completed were found to be very similar on each injector. They were characterized by a thin, uneven layer covering the front surface of the atomizer with local clusters of sediments of various sizes and thickness. Only in the area of the central convexity of the atomizer tip visible could thickening of homogeneous deposits be found, especially around the fuel outlet openings. These deposits overlapped with the edges of the fuel outflow holes. In the case of the RF-12-09 fuel + 20% (v/v) ethanol (Figure 5, bottom row), deposits around the outflow holes were visibly smaller.

Rapid fluctuations and changes in the fuel injection time were observed during the tests. Such fluctuations during injector operation are thought to be the result of simultaneous processes of injector contamination (formation of deposits) and their cleaning, i.e., deposits were formed and then periodically broke off and flew out. Such a phenomenon was already known to take place, for example, in the case of deposits on the engine inlet valves [28]. It was deemed important to note that in the case of the RF-12-09 fuel without ethanol, the increase in fuel injection time increased linearly throughout the test duration. It could be hypothesized that, if the test time was extended, the fuel injection time would further increase and, therefore, the deposits on the tips and in the fuel injector outlet holes would also increase. Another trend of changes in the fuel injection time was noted during the tests for fuels containing ethanol admixtures. For these fuels, the observed fuel injection time change during the test was logarithmic. Consequently, after a period of rapid, progressive increase in fuel injection time, it was stabilized over time at a certain level. In the case of the RF-12-09 fuel containing ethanol, such stabilization took place after 25–30 h from the start of the test. It was therefore possible that past this point in time, when the changes in fuel injection time stabilized, the total size of the deposits was more influenced by the processes of their removal, and less by the processes of their formation. This would explain the clearly smaller and less uniform deposits around the outlet openings in the area of the central convexity of the atomizer tip in the case of the test conducted using the RF-12-09 + 20% (v/v) ethanol fuel (Figure 5).

The differences in the deposits' formation process and their size on injectors using the tested fuels resulted from the intensity of the deposit precursor formation processes, the force of their adhesion to the surfaces on which they were formed, and the simultaneous processes of self-cleaning of the injectors. The logarithmic nature of the sediment buildup on the injectors indicated a greater speed of the sediment precursor formation process at the beginning of the injector operation, stronger adherence to the surface, and/or reduced intensity of the deposits' removal (washing) from the surface. For a linear characteristic, the sediment formation and removal processes take place with a constant intensity in a certain proportion to one another, with the buildup of injector deposits winning out slightly. After the formation and stabilization of sediment precursors on the surface of the injectors, further contamination of the injectors was the result of the sediment buildup and removal processes. The results obtained in this study were inconsistent with those described in [24,25], but in line with the results described in [27].

Limiting the fuel injectors' deposit formation during engine operation when using ethanol-containing fuels could enable reductions in both exhaust emissions of harmful components to the atmosphere and emissions of CO_2. This would be the result of the better (compared to ethanol-free fuels) fuel atomization process in the air of the cylinder. Thus, a more effective process of creating a combustible mixture in the required form (homogeneous or layered) could be achieved, leading to a more complete combustion process. Overall, this makes it easier to maintain the desired engine parameters, including the exhaust emissions declared by the manufacturer. Thus, gasoline fuels containing alcohol in their composition have a greater pro-ecological potential compared to gasoline without an alcohol admixture.

Analysis of the fuel atomization indicators for high-pressure injectors in a constant volume chamber (Figure 16), taking into account the averaging of the results, allowed us to draw the following conclusions:

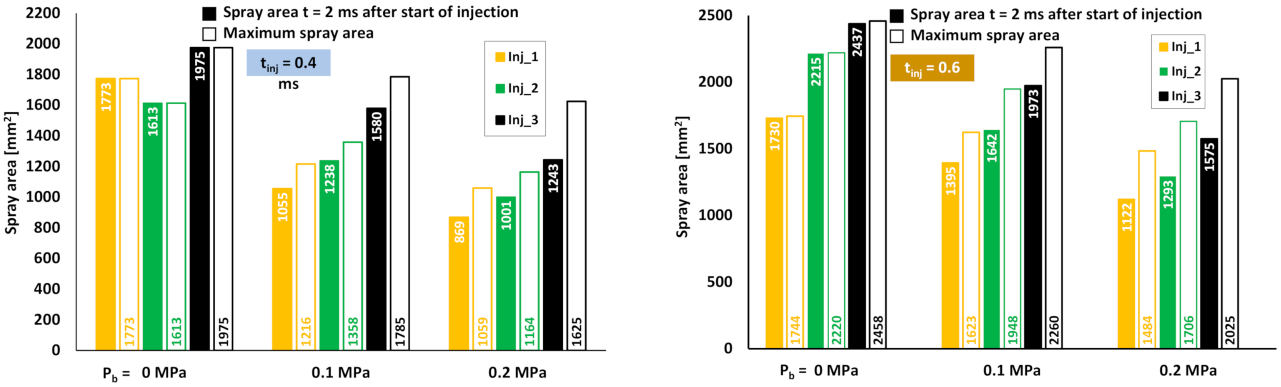

Figure 16. Summary of the averaged maximum recorded fuel spray area and the area achieved after 2 ms for tests using the injectors after the test run with the RF-12-09 fuel and fuels with ethanol admixture: (**a**) with injection time t = 0.4 ms; (**b**) with injection time t = 0.6 ms.

- Having no back pressure in the chamber resulted in a slight difference between the maximum fuel spray surface area achieved and that observed within 2 ms after the start of injection;
- Increasing the back pressure increased the differences between the two analytical points; in measurements carried out at a back pressure of 0.1 MPa, the maximum spray area was approximately 12% greater than that achieved after 2 ms. In tests carried out with a backpressure of 0.2 MPa, this difference was about 25%;
- At all measurement points, the highest spray area was obtained in the tests of injectors previously operating with the RF-12-09 + 20% ethanol fuel.

In most studies, the smallest surface area was obtained on injectors previously operating with the RF-12-09 reference fuel.

5. Conclusions

1. Each SI engine design, influencing the combustion process strategy by the design of the injectors, has a very large impact on the intensity of the injector coking phenomenon. Hence, the final result of the fuel assessment in terms of the effect on deposit formation and the size of the deposits generated in a given time.
2. All of the changes in fuel injection time (tests in the VW EA111 BLG engine) obtained as part of the fuel tests carried out in the course of the research were characterized by a gradual increase—often very variable in time. This indicates the simultaneous occurrence of injector contamination and cleaning processes.

3. Variations in the injector deposit formation trends when using the tested fuels resulted from the intensity of the deposit precursor formation processes and the force of their adhesion to the surface of the injector, as well as the intensity of the deposit growth, and were then opposed by the simultaneous processes of the injectors' self-cleaning due to fuel flow.
4. Extensive research on qualitative indicators of fuel atomization for high-pressure injectors in a constant volume chamber allowed for the analysis of changes in their operational parameters for test cases injecting fuels with and without an alcohol admixture.

Author Contributions: Conceptualization, Z.S., I.P., F.S. and W.C.; methodology, Z.S., F.S. and I.P.; software, I.P. and F.S.; validation, Z.S., F.S. and W.C.; formal analysis, F.S. and W.C.; investigation, Z.S., I.P., F.S. and W.C.; resources, Z.S.; data curation, Z.S.; writing—original draft preparation, Z.S., F.S., I.P. and W.C.; writing—review and editing, I.P. and F.S.; visualization, F.S. and W.C.; supervision, Z.S.; project administration, Z.S. and I.P. All authors have read and agreed to the published version of the manuscript.

Funding: This research received no external funding.

Institutional Review Board Statement: Not applicable.

Informed Consent Statement: Not applicable.

Data Availability Statement: Not applicable.

Conflicts of Interest: The authors declare no conflict of interest.

References

1. Directive 2003/30/EC of the European Parliament and of the Council of 8 May 2003 on the Promotion and the Use of Biofuels or Other Renewable Fuels for Transport. Available online: https://eur-lex.europa.eu/eli/dir/2003/30/oj (accessed on 2 March 2022).
2. Renewable Energy Directive (RED II). Directive (EU) 2018/2001 (recast) on the promotion of the use of energy from renewable sources. Available online: https://eur-lex.europa.eu/eli/dir/2018/2001/oj (accessed on 2 March 2022).
3. Worldwide Fuel Charter—2019 (Fifth Edition). Available online: https://www.acea.auto/files/WWFC_19_gasoline_diesel.pdf (accessed on 3 March 2022).
4. Sarathy, S.M.; Oβwald, P.; Hansen, N.; Kohse-Höinghaus, K. Alcohol combustion chemistry. *Prog. Energ. Combust.* **2014**, *44*, 40–102. [CrossRef]
5. Balki, M.; Sayin, C.; Canakci, M. The effect of different alcohol fuels on the performance, emission and combustion characteristics of a gasoline engine. *Fuel* **2014**, *115*, 901–906. [CrossRef]
6. Fourier, E.; Simon, G.; Seers, P. Evaluation of low concentrations of ethanol, buthanol BE, and ABE with gasoline direct-injection, spark-ignition engine. *Fuel* **2016**, *181*, 396–407. [CrossRef]
7. Badawy, T.; Attar, M.A.; Xu, H.; Ghafourian, A. Assessment of gasoline direct injector fouling effects on fuel injection, engine performance and emission. *Appl. Energy* **2018**, *220*, 351–374. [CrossRef]
8. Elfasakhany, E. Performance and emissions of spark-ignition engine using ethanol-methanol-gasoline, n-butanol-iso-butanol-gasoline and iso-butanol-ethanol gasoline blends. *Eng. Sci. Technol. Int. J.* **2016**, *19*, 2053–2059. [CrossRef]
9. Shuai, S.; Ma, X.; Li, Y.; Qi, Y.; Xu, H. Recent progress in automotive gasoline direct injection engine technology. *Automot. Innov.* **2018**, *1*, 95–113. [CrossRef]
10. Mengzhao, C.; Jeonghyun, P.; Byunggyun, K.; Jeong, H.P.; Park, S.; Suhan, P. Effect of sac-volume on the relationship among ball behavior, injection and initial spray characteristics of ultra-high pressure GDI injector. *Fuel* **2020**, *285*, 119089. [CrossRef]
11. Henkel, S.; Hardalupas, Y.; Taylor, A.; Conifer, C.; Cracknell, R.; Kit Goh, T.; Reinicke, P.-B.; Sens, M.; Rieß, M. Injector fouling and its impact on engine emissions and spray characteristics in gasoline direct injection engines. *SAE Int. J. Fuels Lubr.* **2017**, *10*, 287–295. [CrossRef]
12. Czerwinski, J.; Comte, P.; Stepien, Z.; Oleksiak, S. Effects of ethanol blend fuels E10 and E85 on the non-legislated emissions of a flex fuel passenger car. In *SAE Technical*; SAE International: Warrendale, PA, USA, 2016. [CrossRef]
13. Xu, H.; Wang, C.; Ma, X.; Sarangi, A.K.; Weall, A.; Krueger-Venus, J. Fuel injector deposits in direct-injection spark-ignition engines. *Prog. Energy Combust.* **2015**, *50*, 63–80. [CrossRef]
14. Wang, B.; Badawy, T.; Jiang, Y.; Xu, H.; Ghafourian, A.; Hang, X. Investigation of deposit effect on multi-hole injector spray characteristics and air/fuel mixing process. *Fuel* **2017**, *191*, 10–24. [CrossRef]
15. Stępień, Z.; Żak, G.; Markowski, J.; Wojtasik, M. Investigation into the impact of the composition of ethanol fuel deposit control additives on their effectiveness. *Energies* **2021**, *14*, 604. [CrossRef]
16. Pielecha, I.; Skowron, M.; Mazanek, A. evaluation of the injectors operational wear process based on optical fuel spray analysis. *Eksploat. Niezawodn.* **2018**, *20*, 83–89. [CrossRef]

17. Leach, F.; Knorsch, T.; Laidig, C.; Wiese, W. A review of the requirements for injection systems and the effects of fuel quality on particulate emissions from GDI engines. In *SAE Technical*; SAE International: Warrendale, PA, USA, 2018. [CrossRef]
18. Awad, O.; Xiao, M.; Kamil, M.; Zhou, B.; Ali, O.M.; Shuai, S. A review of the effects of gasoline detergent additives on the formation of combustion chamber deposits of gasoline direct injection engines. *SAE Int. J. Fuels Lubr.* **2021**, *14*, 13–25. [CrossRef]
19. Barker, J.; Reid, J.; Mulqueen, S.; Langley, G.J.; Wilmot, E.M.J.; Vadodaria, S.; Castle, J.; Whitaker, J. The investigation of the structure and origins of gasoline direct injection (GDI) deposits. In *SAE Technical*; SAE International: Warrendale, PA, USA, 2019. [CrossRef]
20. Wetzel, J. Optical analysis of the influence of injector hole geometry on mixture formation in gasoline direct injection engines. *Automot. Engine Technol.* **2016**, *1*, 57–67. [CrossRef]
21. Chan, Q.N.; Bao, Y.; Kook, S. Effects of injection pressure on the structural transformation of flash-boiling sprays of gasoline and ethanol in a spark-ignition direct-injection (SIDI) engine. *Fuel* **2014**, *130*, 228–240. [CrossRef]
22. Jiang, C.; Xu, H.; Srivastava, D.; Ma, X.; Dearn, K.; Cracknell, R.; Krueger-Venus, J. Effect of fuel injector deposit on spray characteristics, gaseous emissions and particulate matter in a gasoline direct injection engine. *Appl. Energy* **2017**, *203*, 390–402. [CrossRef]
23. Zhang, W.; Zhang, Z.; Ma, X.; Awad, O.I.; Li, Y.; Shuai, S.; Xu, H. Impact of injector tip deposits on gasoline direct injection engine combustion, fuel economy and emissions. *Appl. Energy* **2020**, *262*, 114538. [CrossRef]
24. Bueschke, W.; Szwajca, F.; Wislocki, K. Experimental study on ignitability of lean CNG/air mixture in the multi-stage cascade engine combustion system. In *SAE Technical*; SAE International: Warrendale, PA, USA, 2020. [CrossRef]
25. Pielecha, I. Fuel injection rate shaping and its effect on spray parameters in a direct-injection gasoline system. *J. Vis.* **2022**. [CrossRef]
26. Stępień, Z.; Pielecha, I.; Cieslik, W.; Szwajca, F. The impact of alcohol admixture with gasoline on carbon build-up and fuel injectors performance. *Eksploat. Niezawodn.* **2022**, *24*, 226–236. [CrossRef]
27. Pielecha, I.; Maslennikov, D.; Wislocki, K. Optical research of spray development of E85 fuel in high pressure gasoline direct injection system. In *SAE Technical*; SAE International: Warrendale, PA, USA, 2010. [CrossRef]
28. Stępień, Z. Deposit in spark ignition engines—Formation and threats. *Comb. Eng.* **2015**, *160*, 36–48. [CrossRef]